

Two-Component Gelators and Nucleating Agents for Polypropylene Based upon Supramolecular Assembly

Thorsten Bauer, Ralf Thomann, and Rolf Mülhaupt*

Freiburger Materialforschungszentrum und Institut für Makromolekulare Chemie der Albert-Ludwigs Universität, Stefan-Meier-Str. 21, D-79104 Freiburg i.Br., Germany

Received May 21, 1998; Revised Manuscript Received July 29, 1998

ABSTRACT: The supramolecular assembly of octyl-, hexadecyl-, and benzyl-substituted complementary tectonics based upon barbiturates (BA) and 2,4,6-triaminopyrimidines (TP) were studied in bulk, in cyclohexane, and in a polypropylene matrix. As evidenced by means of wide-angle X-ray scattering, FTIR spectroscopy, and atomic force microscopy (AFM), BA/TP assembly led to the formation of nanofibrillated superstructures, whereas the individual BA and TP components exhibited layered superstructures. Nanostructure formation resulting from BA/TP assembly in polypropylene melt accounted for nucleation of polypropylene crystallization, especially when using benzyl-substituted BA and TP derivatives instead of the corresponding *n*-alkyl-substituted derivatives. As a function of the benzyl ring substitution pattern it was possible to vary interlayer spacing and to influence nucleation with optimum nucleation efficiency observed for 1.61 nm spacing in the case of MeBz-BA/Bz-TP. Injection molding in the presence of MeBz-BA/Bz-TP and of Bz-BA/MeBz-TP assemblies revealed increased stiffness, as determined by Young's modulus, without sacrificing impact strength when the content of nucleating assembly was increased from 0 to 2 wt %. Transcrystallization of polypropylene onto BA/TP nanostructures was imaged by means of crossed-polarized light microscopy.

Introduction

Recent innovations in supramolecular chemistry have stimulated new developments of nanostructured polymeric materials, which have benefited from fruitful interdisciplinary efforts of macromolecular, supramolecular, and colloid chemistry. Supramolecular assemblies represent an important novel approach to complex molecular and supermolecular architectures. The exciting potential of supramolecular self-assemblies leading to programmed supramolecular systems was reviewed by Lehn.¹ Supramolecular self-assembly is based upon the spontaneous recognition-driven association of small molecules which function as supermolecular monomers and are referred to by Wuest as "tectonics" (from Greek "τεκτων" for builder).^{2,3}

Supramolecular polymers represent a recent development in this area. These polymers—unlike conventional polymers, which are built by covalent linking of monomers—linear, branched, cyclic, helical, fiberlike, ladderlike, gridlike, and sheetlike polymers and networks can be designed by exploiting the formation of hydrogen bridges between complementary donor/acceptor-type monomers. Recently, Meijer's group reported bifunctional tectonics containing an array of four parallel hydrogen groups in the 2-ureido-4-pyrimidone moiety, which accounts for step growth formation of the corresponding linear supramolecular polymer.⁴ Such polymers simultaneously exhibit properties typical for small molecules and high molecular weight polymers. Due to the presence of hydrogen bridges in the backbone, polymers exhibiting high solution viscosity are cleaved at elevated temperature to yield the corresponding monomers having low viscosity. Although this reversible behavior may facilitate processing, dynamic disassembling and reassembling account for lower stiffness with respect to conventional polymers containing

covalent bonds between monomeric units. Several groups report the use of supramolecular assemblies to produce nanostructured gels in bulk and in organic and aqueous media as recently reviewed by Terech and Weiss.⁵

Much less attention is devoted to self-assembly of tectonics in a continuous cross-linked or thermoplastic polymer matrix as an attractive route to achieve nanostructure formation in polymer matrixes. In fact, supramolecular nanostructure formation is of great industrial significance and plays a key role in nucleation of polypropylene melt crystallization, e.g., in the presence of dibenzylidene sorbitol and its derivatives, which are well-known nucleating agents and clarifiers useful in polypropylene melt processing.^{6–10} Shepard and co-workers⁶ identified gel formation via three-dimensional self-assembly of dibenzylidene sorbitol, leading to connected nanofibrils within the polypropylene matrix. Similar results for dibenzylidene sorbitol in a PEO matrix were reported earlier by Thierry and co-workers.³² Such nucleating agents improve stiffness and optical clarity of polypropylene due to reduced spherulite size. Rapid crystallization at elevated temperatures in the presence of nucleating agents accounts for improved processing in injection molding.^{7–10} Although empirical efficiency scales and modeling approaches have been reported, there is much to be learned about the role of superstructures and surface composition in nucleation.

An objective of this research was the investigation of nanostructure formation achieved by means of supramolecular self-assembly of tectonics based upon substituted barbiturates combined with complementary derivatives of 2,4,6-triaminopyrimidines. Self-assembly in bulk, organic media, and polypropylene melts was examined as a function of the substitution patterns of these tectonics. Special emphasis was placed upon examining the influence of nanostructure formation on crystallization, morphology, and mechanical properties of polypropylene.

* To whom correspondence should be addressed.

Experimental Section

General Procedures. All manipulations were performed using standard Schlenck and vacuum line techniques. Reactions were carried out in a three-neck round-bottom flask equipped with magnetic stirrer, gas inlet adapters, dropping funnel, and condenser.

Materials. Malononitrile, diethyl malonate, 1-bromo-octane, sodium and sodium hydride (all obtained from Aldrich), diethyl 2-benzylmalonate, 1-bromohexadecane, benzaldehyde, 4-methyl- and 4-ethylbenzaldehyde (obtained from Fluka), and xylene (isomeric mixture), urea and guanidine hydrochloride (obtained from E. Merck) were used as received. Ethanol absolute (Riedel-de Haën) and dimethyl sulfoxide (E. Merck) were dried and freshly distilled prior to use.

Dibenzylidenesorbitol (DBS) from Milliken Chemical and bis(*p*-ethylbenzylidene)sorbitol (EDBS, NC4) from Mitsui Toatsu Chem. were used as received. The isotactic Ziegler-based polypropylene KY 6100 supplied by Shell Chemical Co. was of commercial grade used without further purification. The weight average mass is 285,900 g/mol, M_w/M_n is 4.9. The polypropylene melts at 165.8 °C and crystallizes at 113.0 °C as measured by DSC (rate 10 °C/min). The tacticity is 97% isotactic determined by ^{13}C NMR triad distribution.

Characterization. ^1H and ^{13}C NMR were recorded on a Bruker ARX 300 spectrometer at 300 and 75.41 MHz, respectively. All spectra were obtained at room temperature, and chemical shifts are quoted in parts per million (ppm). All deuterated solvents were purchased from Aldrich and were used as received. IR spectra were recorded on a Perkin-Elmer 1330 IR; FTIR spectra were obtained from a Bruker IFS88. Melting points are given as maximum peaks of DSC runs (Perkin-Elmer DSC-7) at a rate of 10 °C/min. Elementary analysis was performed on a Perkin-Elmer 240 Elemental Analyzer.

Preparation of Tectonics. 2-Octylmalononitrile. Similar to reported procedures^{11,12} 18.36 g (17.5 mL, 0.28 mol) of malononitrile were dissolved in 45 mL of DMSO, and the solution was added to a stirred slurry of 6.70 g (0.28 mol) of sodium hydroxide in 200 mL of DMSO within a period of 1 h under occasional cooling with an ice bath to maintain a temperature of 20–25 °C. After the gas evolution had finished, 54.04 g (48.5 mL, 0.28 mol) of 1-bromooctane was added under constant stirring within a period of 20 min while maintaining the temperature of 20–25 °C (occasional cooling with an ice bath). After 3 h of stirring the reaction mixture was poured into 200 mL of ice cold water. The resulting solution was extracted three times with 75 mL of diethyl ether, and the organic phases were dried over magnesium sulfate, filtered, and distilled after removing of the solvent to give two fractions: (1) 145–148 °C/0.5 mbar, 26.62 g (53%) (product) and (2) 180–185 °C/0.5 mbar, 2.07 g (disubstituted malononitrile as determined by NMR). Yield: 26.62 g (53%) of a colorless liquid. Bp: 145 °C/0.5 mbar. IR (film): 725, 1380, 1470, 1735, 2260, 2860, 2930, 2960 cm^{-1} . ^1H NMR (CDCl_3): 0.90 (t, 3H, $^3J_{\text{HH}'} = 8.4$ Hz, $-\text{CH}_3$), 1.18–1.46 (m, 10H, $\text{CH}_3(\text{CH}_2)_5-$), 1.62 (m, 2H, $\text{CH}_3(\text{CH}_2)_5\text{CH}_2-$), 2.04 (m, 2H, $\text{CH}_3(\text{CH}_2)_5\text{CH}_2\text{CH}_2-$), 3.72 (t, 1H, $^3J_{\text{HH}'} = 7.2$ Hz, CH). ^{13}C NMR (CDCl_3): 14.0 ($-\text{CH}_3$), 22.5 (CH), 22.6–31.6 (7s, $-(\text{CH}_2)_7-$), 112.6 ($-\text{CN}$). Anal. Calcd for $\text{C}_{11}\text{H}_{18}\text{N}_2$: C, 74.11; H, 10.18; N, 15.71. Found: C, 73.98; H, 9.91; N, 15.65.

2-Hexadecylmalononitrile. The reaction was conducted as above using 13.20 g (0.20 mol) of malononitrile dissolved in 30 mL of DMSO and 5.00 g (0.21 mol) of sodium hydride in 200 mL of DMSO. To this mixture was added 61.02 g (61.0 mL, 0.20 mol) of 1-bromohexadecane. After the reaction mixture was poured into water, the resulting precipitate was filtered, washed twice with 100 mL of water and recrystallized in 200 mL of ethanol. At 50 °C fine white needles precipitated (disubstituted malononitrile as determined by NMR) which were removed. Cooling of the mother liquor with an ice bath gave the desired product, white needles, which were filtered and dried. Yield: 18.50 g (32%). Mp: 59 °C. IR (KBr): 720, 730, 1140, 1380, 1405, 1440, 1470, 1710, 2260, 2860, 2930, 2960 cm^{-1} . ^1H NMR (CDCl_3): 0.90 (t, 3H, $^3J_{\text{HH}'} = 8.4$ Hz,

$-\text{CH}_3$), 1.21–1.42 (m, 26H, $\text{CH}_3(\text{CH}_2)_{13}-$), 1.65 (m, 2H, $\text{CH}_3(\text{CH}_2)_{13}\text{CH}_2-$), 2.05 (m, 2H, $\text{CH}_3(\text{CH}_2)_{13}\text{CH}_2\text{CH}_2-$), 3.72 (t, 1H, $^3J_{\text{HH}'} = 7.2$ Hz, CH). ^{13}C NMR (CDCl_3): 14.0 ($-\text{CH}_3$), 22.1 (CH), 22.2–31.9 (15s, $-(\text{CH}_2)_{15}-$), 112.0 ($-\text{CN}$). Anal. Calcd for $\text{C}_{19}\text{H}_{34}\text{N}_2$: C, 78.56; H, 11.80; N, 9.64. Found: C, 78.62; H, 11.89; N, 9.43.

2-Benzylidenemalononitrile. Synthesis was performed according to literature procedures.¹³ Yield: 68%. Mp: 86 °C (lit.¹³ mp 86 °C).

2-(4-Methylbenzylidene)malononitrile. Yield: 86%. Mp: 134 °C (lit.¹³ mp 135 °C).

2-(4-Ethylbenzylidene)malononitrile. Yield: 61%. Mp: 76 °C.

2-Benzylmalononitrile. The reduction reactions of unsaturated malononitriles were performed as described by Nanjo.¹⁴ Yield: 68%. Mp: 91 °C (lit.¹⁵ mp 91 °C).

2-(4-Methylbenzyl)malononitrile. Yield: 88%. Mp: 84 °C (lit.¹⁵ mp 84 °C).

2-(4-Ethylbenzyl)malononitrile. Yield: 73%. Mp: 73 °C.

5-Octyl-2,4,6-triaminopyrimidine (O-TP). (IUPAC: 5-Octyl-2,4,6-pyrimidinetriamine.) The formation of 2,4,6-triaminopyrimidines was achieved by the route of Russell¹⁶ using the appropriate malononitrile (0.1 mol) and guanidine hydrochloride (0.12 mol) in sodium (0.15 mol)/ethanol (200 mL). After refluxing for 5 h, the mixture was filtered hot to remove the sodium chloride formed. The solution was allowed to cool, which resulted in crystallization of the triaminopyrimidine. Recrystallization from ethanol yielded the colorless product. Yield: 63%. Mp: 132 °C (lit.¹⁷ mp 132–133 °C). IR (KBr): 640, 790, 825, 1020, 1080, 1260, 1425, 1465, 1485, 1575–1655, 2850, 2920, 3190, 3380, 3490, cm^{-1} . ^1H NMR (CDCl_3): 0.88 (t, 3H, $^3J_{\text{HH}'} = 8.4$ Hz, $-\text{CH}_3$), 1.18–1.40 (m, 10H, $\text{CH}_3(\text{CH}_2)_5-$), 1.49 (m, 2H, $\text{CH}_3(\text{CH}_2)_5\text{CH}_2-$), 2.21 (t, 2H, $^3J_{\text{HH}'} = 9.6$ Hz, $\text{CH}_3(\text{CH}_2)_5\text{CH}_2\text{CH}_2-$), 4.41 (s, 6H, $-\text{NH}_2$) ppm. ^{13}C NMR (CDCl_3): 14.0 ($-\text{CH}_3$), 22.6–31.6 (7s, $-(\text{CH}_2)_7-$), 88.3 ($\text{C}_8\text{H}_{17}\text{C}-$), 160.6 (2-CNH₂), 161.9 (4,6-CNH₂) ppm. Anal. Calcd for $\text{C}_{12}\text{H}_{23}\text{N}_5$: C, 60.73; H, 9.77; N, 29.50. Found: C, 60.67; H, 9.74; N, 29.54.

5-Hexadecyl-2,4,6-triaminopyrimidine (H-TP). Yield: 72%. Mp: 127 °C. IR (KBr): 635, 785, 810, 1075, 1415, 1455, 1475, 1560–1645, 2815, 2900, 3180, 3365, 3480 cm^{-1} . ^1H NMR (CDCl_3): 0.86 (t, 3H, $^3J_{\text{HH}'} = 8.4$ Hz, $-\text{CH}_3$), 1.24 (m, 26H, $\text{CH}_3(\text{CH}_2)_{13}-$), 1.46 (m, 2H, $\text{CH}_3(\text{CH}_2)_{13}\text{CH}_2-$), 2.20 (t, 2H, $^3J_{\text{HH}'} = 9.6$ Hz, $\text{CH}_3(\text{CH}_2)_{13}\text{CH}_2\text{CH}_2-$), 4.41 (s, 6H, $-\text{NH}_2$) ppm. ^{13}C NMR (CDCl_3): 14.1 ($-\text{CH}_3$), 22.7–31.9 (15s, $-(\text{CH}_2)_{15}-$), 86.2 ($\text{C}_{16}\text{H}_{33}\text{C}-$), 160.4 (2-CNH₂), 161.8 (4,6-CNH₂) ppm. Anal. Calcd for $\text{C}_{20}\text{H}_{39}\text{N}_5$: C, 68.72; H, 11.25; N, 20.03. Found: C, 68.84; H, 11.16; N, 19.91.

5-Benzyl-2,4,6-triaminopyrimidine (Bz-TP). Yield: 87%. Mp: 191 °C (lit.¹⁶ mp 191 °C). IR (KBr): 520, 690–805, 1020, 1215, 1430–1480, 1560, 1600, 2820, 2900, 3160, 3370, 3430 cm^{-1} . ^1H NMR ($\text{DMSO}-d_6$): 3.52 (s, 2H, $-\text{CH}_2-$), 5.14 (s, 2H, 2-CNH₂), 5.40 (s, 4H, 4,6-CNH₂), 7.00–7.20 (m, 5H, Ph) ppm. ^{13}C NMR ($\text{DMSO}-d_6$): 28.6 (PhCH₂), 85.0 (PhCH₂C), 125.7, 128.1, 128.2, 141.3 (Ph), 161.3 (2-CNH₂), 162.6 (4,6-CNH₂) ppm. Anal. Calcd for $\text{C}_{11}\text{H}_{13}\text{N}_5$: C, 61.38; H, 6.09; N, 32.53. Found: C, 61.17; H, 6.26; N, 32.46.

5-(4-Methylbenzyl)-2,4,6-triaminopyrimidine (MeBz-TP). Yield: 66%. Mp: 208 °C (lit.¹⁸ mp 208 °C). IR (KBr): 490, 565, 635, 790, 885, 1025, 1100, 1210, 1275, 1290, 1425, 1440, 1480, 1505, 1560–1655, 2920, 3140, 3200, 3340, 3370, 3430, 3480 cm^{-1} . ^1H NMR ($\text{DMSO}-d_6$): 2.23 (s, 3H, CH_3Ph), 3.53 (s, 2H, $-\text{CH}_2-$), 5.22 (s, 2H, 2-CNH₂), 5.43 (s, 4H, 4,6-CNH₂), 6.95–7.15 (m, 4H, Ph) ppm. ^{13}C NMR ($\text{DMSO}-d_6$): 20.8 (CH_3Ph), 28.2 (PhCH₂), 85.2 (PhCH₂C), 128.1, 128.7, 134.5, 138.1 (Ph), 161.2 (2-CNH₂), 162.6 (4,6-CNH₂) ppm. Anal. Calcd for $\text{C}_{12}\text{H}_{15}\text{N}_5$: C, 62.86; H, 6.59; N, 30.55. Found: C, 62.77; H, 6.55; N, 30.42.

5-(4-Ethylbenzyl)-2,4,6-triaminopyrimidine (EtBz-TP). Yield: 87%. Mp: 157 °C. IR (KBr): 480, 565, 630, 790, 835, 885, 1025, 1105, 1210, 1280, 1425, 1445, 1480, 1510, 1570–1655, 2920, 2970, 3140, 3200, 3345, 3380, 3440, 3490 cm^{-1} . ^1H NMR ($\text{DMSO}-d_6$): 1.11 (t, 3H, $^3J_{\text{HH}'} = 7.6$ Hz, CH_3-), 2.53 (m, 2H, CH_3CH_2-), 3.51 (s, 2H, $\text{CH}_3\text{CH}_2\text{PhCH}_2-$), 5.15 (s, 2H, 2-CNH₂), 5.36 (s, 4H, 4,6-CNH₂), 6.98–7.10 (m, 4H, Ph) ppm.

^{13}C NMR (DMSO- d_6): 16.1 (CH_3), 27.9 (CH_3CH_2), 28.2 ($\text{CH}_3\text{-CH}_2\text{PhCH}_2$), 85.3 (PhCH_2C), 125.5, 128.1, 138.4, 141.0 (Ph), 161.2 (2-CNH $_2$), 162.6 (4,6-CNH $_2$) ppm. Anal. Calcd for $\text{C}_{13}\text{H}_{17}\text{N}_5$: C, 64.17; H, 7.04; N, 28.79. Found: C, 64.01; H, 6.97; N, 28.85.

Diethyl 2,2-Dialkylmalonates. Synthesis of dialkylated diethyl malonates with long alkyl chains were done according to the usual method described by Staudinger,¹⁹ Wong,²⁰ Rosatzin,²¹ and others. Sodium (0.5 mol) and 0.2 mol of diethyl malonate were used in 300 mL of dry ethanol. Adding 0.4 mol of the appropriate 1-bromoalkane and stirring for 18 h under reflux yielded the dialkylated products, which were distilled or recrystallized.

Diethyl 2,2-Dioctylmalonate. Yield: 39%. Bp: 160 °C (0.1 mbar).

Diethyl 2,2-Dihexadecylmalonate. Yield: 54%. Mp: 40 °C (lit.¹⁹ mp 40 °C).

Diethyl 2-Benzylmalonate was commercially available from Fluka.

Substituted Barbituric Acids (BA). (IUPAC: 2,4,6-(1H,3H,5H)-Pyrimidinetrione.) According to the method described by Fischer²² substituted barbituric acids were obtained from 0.20 mol of the appropriate diethyl malonate with 0.25 mol urea and 0.30 mol sodium in 500 mL of dry ethanol. Acidification and recrystallization yielded the pure products.

5,5-Dioctylbarbituric Acid (O-BA). Yield: 86%. Mp: 102 °C. IR (KBr): 410, 490, 660, 710, 840, 1030, 1175–1375, 1415–1455, 1700–1750, 2840, 2910, 2940, 3090–3200 cm^{-1} . ^1H NMR (DMSO- d_6): 0.88 (t, 6H, $^3J_{\text{HH}}$ = 7.2 Hz, $2 \times -(\text{CH}_2)_7\text{CH}_3$), 0.95–1.32 (m, 24H, $2 \times -\text{CH}_2(\text{CH}_2)_6\text{CH}_3$), 1.86 (m, 4H, $2 \times -\text{CH}_2(\text{CH}_2)_6\text{CH}_3$), 11.50 (br s, 2H, NH) ppm. ^{13}C NMR (DMSO- d_6): 14.1 ($-(\text{CH}_2)_7\text{CH}_3$), 22.2–31.4 (7s, $-(\text{CH}_2)_7-$), 55.2 ($-C((\text{CH}_2)_7\text{CH}_3)_2$), 150.0 (2-C=O), 173.4 (4,6-C=O) ppm. Anal. Calcd for $\text{C}_{20}\text{H}_{36}\text{N}_2\text{O}_3$: C, 68.14; H, 10.29; N, 7.95. Found: C, 68.45; H, 10.47; N, 7.69.

5,5-Dihexadecylbarbituric Acid (H-BA). Yield: 76%. Mp: 110 °C. IR (KBr): 410, 490, 660, 710, 850, 1030, 1130, 1175–1375, 1415–1460, 1580, 1700–1750, 2840, 2910, 2940, 3090–3200 cm^{-1} . ^1H NMR (CDCl_3): 0.88 (t, 6H, $^3J_{\text{HH}}$ = 7.2 Hz, $2 \times -(\text{CH}_2)_{15}\text{CH}_3$), 1.08–1.35 (m, 56H, $2 \times -\text{CH}_2(\text{CH}_2)_{14}-\text{CH}_3$), 1.82 (m, 4H, $2 \times -\text{CH}_2(\text{CH}_2)_{14}\text{CH}_3$), 11.50 (s, 2H, NH) ppm. ^{13}C NMR (CDCl_3): 14.1 ($-(\text{CH}_2)_{15}\text{CH}_3$), 22.7–32.1 (15s, $-(\text{CH}_2)_{15}-$), 60.9 ($-C((\text{CH}_2)_{15}\text{CH}_3)_2$), 149.0 (2-C=O), 172.1 (4,6-C=O) ppm. Anal. Calcd for $\text{C}_{36}\text{H}_{68}\text{N}_2\text{O}_3$: C, 74.95; H, 11.88; N, 4.86. Found: C, 75.03; H, 11.98; N, 4.64.

5-Benzylbarbituric Acid (Bz-BA). Yield: 62%. Mp: 210 °C (lit.²³ mp 210 °C). IR (KBr): 405, 450, 485, 500, 535, 580, 630–760, 870, 1040, 1205, 1335–1375, 1430, 1480, 1580, 1615, 1640, 1695, 1725, 2850, 3070, 3210 cm^{-1} . ^1H NMR (DMSO- d_6): 3.25 (d, 2H, $^2J_{\text{HH}}$ = 4.8 Hz, PhCH_2-), 3.90 (t, 1H, $^3J_{\text{HH}}$ = 4.8 Hz, $\text{PhCH}_2\text{CH}-$), 7.06–7.30 (m, 5H, Ph), 11.20 (br s, 2H, NH) ppm. ^{13}C NMR (DMSO- d_6): 33.5 (PhCH_2-), 49.5 ($\text{PhCH}_2\text{CH}-$), 126.9, 128.5, 129.1, 137.6 (Ph), 150.8 (2-C=O), 170.2 (4,6-C=O) ppm. Anal. Calcd for $\text{C}_{11}\text{H}_{10}\text{N}_2\text{O}_3$: C, 60.55; H, 4.62; N, 12.84. Found: C, 60.35; H, 4.44; N, 12.85.

5-(4-Methylbenzyl)barbituric Acid (MeBz-BA). According to the procedure described by Tate²⁴ 0.2 mol of barbituric acid in 500 mL of water reacted within 3 days at 20 °C with 0.1 mol of 1-(bromomethyl)-4-methylbenzene using 0.1 mol triethanolamine as base. Yield: 65%. Mp: 229 °C (lit.²⁴ mp 229 °C). IR (KBr): 405, 465, 505, 535, 630–715, 790, 805, 845, 890, 1050, 1190, 1210, 1295, 1315, 1330, 1355, 1405, 1435, 1515, 1705, 1735, 2850, 2920, 3030, 3090, 3230 cm^{-1} . ^1H NMR (DMSO- d_6): 2.24 (s, 3H, $-\text{PhCH}_3$), 3.24 (d, 2H, $^2J_{\text{HH}}$ = 4.8 Hz, $\text{CH}_3\text{PhCH}_2-$), 3.85 (t, 1H, $^3J_{\text{HH}}$ = 4.8 Hz, $\text{CH}_3\text{PhCH}_2\text{CH}-$), 6.93–7.12 (m, 4H, Ph), 11.12 (br s, 2H, NH) ppm. ^{13}C NMR (DMSO- d_6): 20.8 (PhCH_3), 33.3 ($\text{CH}_3\text{PhCH}_2-$), 49.6 ($\text{CH}_3\text{PhCH}_2\text{CH}-$), 129.0, 129.1, 134.3, 136.0 (Ph), 150.8 (2-C=O), 170.2 (4,6-C=O) ppm. Anal. Calcd for $\text{C}_{12}\text{H}_{12}\text{N}_2\text{O}_3$: C, 62.06; H, 5.21; N, 12.06. Found: C, 61.87; H, 5.55; N, 11.83.

5-(4-Ethylbenzyl)barbituric Acid (EtBz-BA). 1-(Bromomethyl)-4-ethylbenzene was prepared according to the literature.²⁵ The preparation of 5-(4-ethylbenzyl)barbituric acid was conducted as above. Yield: 61%. Mp: 213 °C. IR (KBr): 405, 510, 545, 570, 665, 690, 750, 770, 805, 830, 855,

1035, 1095, 1120, 1180, 1275, 1305, 1365, 1395, 1425, 1440, 1520, 1575, 1720, 1765, 2580, 2670, 2890, 2940, 2980, 3250 cm^{-1} . ^1H NMR (DMSO- d_6): 1.10 (t, 3H, $^3J_{\text{HH}}$ = 7.6 Hz, PhCH_2CH_3), 2.53 (m, 2H, PhCH_2CH_2), 3.18 (d, 2H, $^2J_{\text{HH}}$ = 4.8 Hz, PhCH_2-), 3.82 (t, 1H, $^3J_{\text{HH}}$ = 4.8 Hz, $\text{PhCH}_2\text{CH}-$), 6.91–7.10 (m, 4H, Ph), 11.12 (br s, 2H, NH) ppm. ^{13}C NMR (DMSO- d_6): 15.7 (PhCH_2CH_3), 27.9 (PhCH_2CH_2), 33.2 ($\text{CH}_3\text{CH}_2\text{PhCH}_2-$), 49.6 ($\text{CH}_3\text{CH}_2\text{PhCH}_2\text{CH}-$), 127.9, 129.0, 134.7, 142.3 (Ph), 150.8 (2-C=O), 170.2 (4,6-C=O) ppm. Anal. Calcd for $\text{C}_{13}\text{H}_{14}\text{N}_2\text{O}_3$: C, 63.40; H, 5.73; N, 11.38. Found: C, 63.56; H, 5.63; N, 11.18.

Self-Assembly and Gelation. 1. Self-Assembly in Bulk. An equimolar mixture of two components was melted on a glass plate at a temperature just above the melting temperatures of the components. The self-assembled product formed immediately.

2. Self-Assembly out of Solution. Equimolar amounts of two components were dissolved in solvents such as CHCl_3 and DMSO. Mixing the solutions yielded a precipitate that was dried after removing of solvent. The self-assembled products were characterized using DSC, FTIR, polarized light microscopy, AFM, and WAXS.

3. Gelation. A total of 0.05 mmol of each component was dissolved in 1 mL of hot cyclohexane in a septum-capped test tube. The resulting 0.1 molar solutions were cooled at 25 °C for several hours. The time was measured, until the formed gel is stable enough so that the tube can be inverted without change of shape of the gel.

Polypropylene Blends. 1. Polypropylene Blends out of Solution. Polypropylene (1 g) and the appropriate amount of an equimolar mixture of two components were dissolved in 50 mL of xylene at 140 °C. Rapid precipitation was achieved by pouring into 100 mL of acetone at its freezing point. This technique is known to produce well-mixed blends.²⁶

2. Melt Blending. Polypropylene extruder blends were prepared in a corotating twin screw extruder (ZSK25, Werner & Pfleiderer) with 300 rpm and processing temperatures between 190 and 230 °C. The extruded materials were injection molded on a Ferromatic Milacron K40-DE at processing temperatures between 200 and 225 °C to obtain specimens for testing of material properties. The temperature of the mold was 50 °C.

Polymer Characterization. 1. Thermal Analysis. Differential scanning calorimetry measurements were performed on a Perkin-Elmer DSC-7. After heating at a rate of 10 °C/min from room temperature to 220 °C (230 °C in the case of MeBzBA) the crystallization temperatures T_c were obtained as endothermic peaks when cooling at a rate of 10 °C/min.

2. Polarized Light Microscopy. An Olympus Vanox AH2 Research Microscope with a Linkam THM 600/TMS 90 hot stage was used.

3. Wide-Angle X-ray Scattering. Layered structures of self-assembled tectonics within and without a polypropylene matrix were determined with a Siemens D 500 X-ray apparatus.

4. Mechanical Properties. Young's moduli (DIN 53455) were measured on an Instron 4202 at a crosshead speed of 1 mm/min between 0.05 and 0.25% strain. Values for yield stress were obtained at a crosshead speed of 50 mm/min. A Zwick 5102 was used to determine notched impact strengths (ISO 180–1, IZOD).

5. Atomic Force Microscopy. AFM experiments were carried out with a Nanoscope III scanning probe microscope from Digital Instruments Inc. at ambient conditions in tapping and contact mode.

Results and Discussion

Among the very large array of modern complementary supramolecular monomers, substituted barbiturates, abbreviated as BA, and substituted 2,4,6-triaminopyrimidines, abbreviated as TP, were selected as tectonics because these compounds are known to form large and stable supramolecular assemblies by the formation of

Table 1. Melting Temperatures of Tectonics and Their Supramolecular Assemblies

sample	R ₁	R ₂	R ₃	T _m (°C)	ΔT _m ^a (°C)
E-BA/B-TP	<i>n</i> -C ₂ H ₅	<i>n</i> -C ₂ H ₅	<i>n</i> -C ₄ H ₉	215 ¹²	19.5
B-BA/B-TP	<i>n</i> -C ₄ H ₉	<i>n</i> -C ₄ H ₉	<i>n</i> -C ₄ H ₉	268 ¹²	88.5
E-BA/O-TP	<i>n</i> -C ₂ H ₅	<i>n</i> -C ₂ H ₅	<i>n</i> -C ₈ H ₁₇	207 ¹²	45.5
B-BA/O-TP	<i>n</i> -C ₄ H ₉	<i>n</i> -C ₄ H ₉	<i>n</i> -C ₈ H ₁₇	215 ¹²	69.5
O-BA/O-TP	<i>n</i> -C ₈ H ₁₇	<i>n</i> -C ₈ H ₁₇	<i>n</i> -C ₈ H ₁₇	171	54.0
H-BA/H-TP	<i>n</i> -C ₁₆ H ₃₃	<i>n</i> -C ₁₆ H ₃₃	<i>n</i> -C ₁₆ H ₃₃	165	46.5
Bz-BA/Bz-TP	C ₆ H ₅ CH ₂ –	H	C ₆ H ₅ CH ₂ –	271	70.5
MeBz-BA/MeBz-TP	CH ₃ C ₆ H ₄ CH ₂ –	H	CH ₃ C ₆ H ₄ CH ₂ –	272	53.5
EtBz-BA/EtBz-TP	C ₂ H ₅ C ₆ H ₄ CH ₂ –	H	C ₂ H ₅ C ₆ H ₄ CH ₂ –	240	55.0
MeBz-BA/Bz-TP	CH ₃ C ₆ H ₄ CH ₂ –	H	C ₆ H ₅ CH ₂ –	265	55.0
Bz-BA/MeBz-TP	C ₆ H ₅ CH ₂ –	H	CH ₃ C ₆ H ₄ CH ₂ –	269	60.0
EtBz-BA/Bz-TP	C ₂ H ₅ C ₆ H ₄ CH ₂ –	H	C ₆ H ₅ CH ₂ –	244	42.0

^a Melting temperature difference between experimental value and that calculated from the individual components, taking into account their mixing ratios.

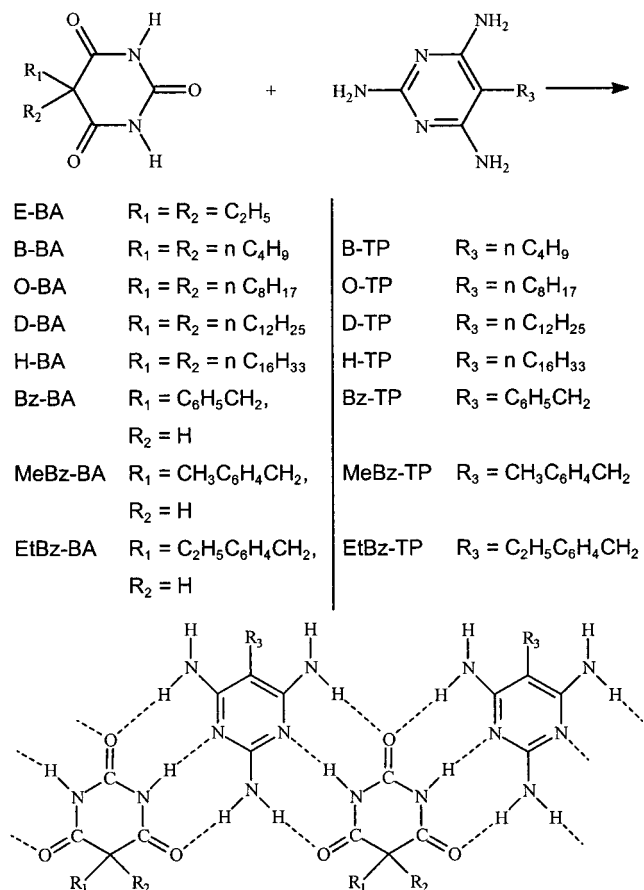


Figure 1. Supramolecular assemblies of BA- and TP-based tectonics.

three H-bonds per molecule.^{1,17} Moreover these tectonics readily melt within a polypropylene melt ($T_m = 165$ °C) at its typical processing temperatures of 220–240 °C, while thermal stability is adequate to sustain these temperatures. The resulting supramolecular assemblies, however, crystallize within the polymer melt far above the recrystallization temperature of polypropylene (which crystallizes at 108–114 °C). Adequate thermal properties, compatibility or easy dispersion, respectively, and thermal stability are important requirements for investigations of supramolecular assemblies of tectonics in polypropylene melts.

A. Formation of Self-Assemblies. Molecular architectures of substituted BA and TP tectonics as well as their supramolecular architectures are displayed in Figure 1. Their melting temperatures, as determined by means of thermal analysis (DSC), are listed in Table

1. Supramolecular assemblies based upon bisuracil/TP²⁷ and substituted BA/TP,¹⁷ using E-BS, B-BS, and O-BS together with E-TP, B-TP, and O-TP, were pioneered by Lehn who observed substantially higher melting temperatures for those assemblies compared to the individual components and was able to identify the crystal structure of E-BS/B-TP thus confirming the general structure displayed in Figure 1. According to Lehn and Whitesides it is possible to replace TP-based tectonics by melamine derivatives to generate similar assemblies.^{28–30}

With long-chain alkyl-substituted BA/TP assemblies, Hanabusa³¹ was able to achieve gel formation in organic media such as cyclohexane. Dodecyl and hexadecyl substituents were used and intertwisting fibers of BA/TP assemblies within a cyclohexane gel were visualized by TEM.

Since most sorbitol-based nucleating agents are substituted with benzylidene groups, benzyl derivatives of BA and TP, Bz-TP and Bz-BA, which have not yet been investigated with respect to their assemblies, were included in this study. Both TP- and BA-based tectonics are readily available. Similar to procedures reported by Bloomfield¹¹ and Beckhaus,¹² malononitrile was alkylated with alkyl halides in dry dimethyl sulfoxide (DMSO) using sodium hydride to generate the sodium salt of malononitrile. Monobenzoylation was performed according to the Knoevenagel condensation using benzaldehydes, described by Milart,¹³ followed by hydrogenation as proposed by Nanjo.¹⁴ Formation of TP was achieved by reacting substituted malononitrile with guanidinium hydrochloride in dry ethanol similar to procedures reported by Russel and Hitchings.¹⁶ The synthetic route to alkyl- and benzyl-substituted BA involved cyclization of the corresponding substituted diethylmalonate with urea, as proposed earlier by Fischer.²²

As is apparent from Table 1, the melting point difference between the experimental melting temperature and theoretical melting temperature, calculated from those of the individual components by taking into account their mixing ratio, increased with decreasing number of C atoms of the alkyl or benzyl substituents, respectively. Assemblies were readily prepared in solution. When the chloroform solutions of the TP and BA were mixed together, the (1:1) assemblies precipitated because TP/BA assemblies were much less soluble.

Hanabusa reported of the formation of gels when cooling the mixture of hot cyclohexane solutions of dodecyl- and hexadecyl-substituted BA and TP resulted in the formation of the assemblies. Hanabusa used FTIR, TEM and WAXS measurements to support the

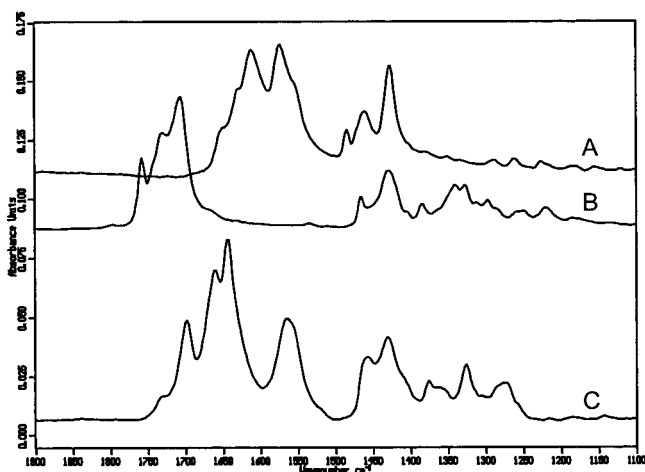


Figure 2. FTIR spectra of O-TP (A), O-BA (B), and O-BA/O-TP assembly (C).

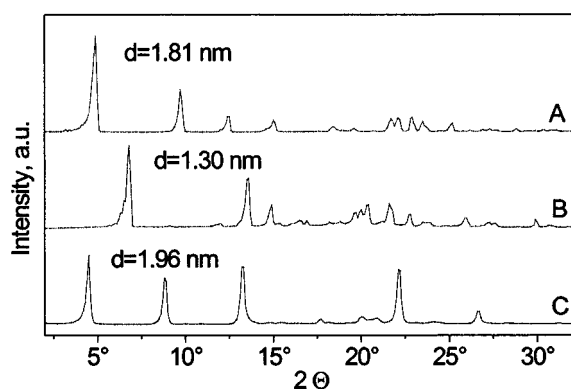


Figure 3. WAXS traces of O-TP (A), O-BA (B), and O-BA/O-TP (C), which was prepared by melt blending.

formation of layered, nanofibrillated structures for the resulting assemblies.³¹ Using the method of Hanabusa, we also employed octyl-substituted TP and BA, e.g., O-BA/O-TP, H-BA/O-TP, O-BA/H-TP successfully to form assemblies similar to those of H-BA/H-TP reported by Hanabusa. In fact, upon cooling a 0.1 mol/L cyclohexane solution of O-BA/O-TP only 5–8 min were required to afford gels in contrast to 90 min for H-TP/H-BS-based gels. Due to their insolubility in cyclohexane, both Bz-TP and Bz-BA were not applied to prepare cyclohexane gels. In bulk, an exothermic peak of the DSC, following melting of one of the components, indicated crystallization of the assembly, which melted at higher temperatures (cf., Table 1). The rearrangement of H-bridges is clearly visible when recording the FTIR spectra of O-TP, O-BA, and O-BA/O-TP, which are displayed in Figure 2. A typical feature of assemblies is the presence of an absorption at 1650 cm^{-1} , which corresponds to the valence vibration of $\text{C}=\text{O}\cdots(\text{H}-\text{N})$.

Also the superstructures of O-BA/O-TP, prepared by melt blending, were markedly different from those of the individual components. Figure 3 depicts the WAXS traces of O-BA/O-TP prepared by melt blending of O-BA and O-TP and for comparison the WAXS traces of O-BA and O-TP. There are always some small reflections that can be related to the inner structure of the respective crystals, and in each case an intense peak at small angles, that can be related to a layered superstructure. The interlayer distance of the O-BA/O-TP is 1.96 nm with respect to 1.81 nm for O-TP and only 1.30 nm for O-BA. These layered structures were confirmed by

AFM studies. Both O-TP and O-BA were melt blended between two glass plates. After removing one glass plate, the surface was scanned with AFM. Figure 4A depicts AFM tapping mode micrographs of O-TP. The height mode image (left) shows that the crystal morphology of O-TP is formed by broad layers. The amplitude mode micrograph (right) shows this structure in more detail. The interlayer distance measured by AFM is about 1.85. This value is in very good agreement to the WAXS measurements given above. Figure 4B shows a contact deflection mode AFM micrograph of O-BA/O-TP. In contrast to O-TP (and O-BA) O-BA/O-TP forms needlelike layers. This fibrillated layered structure is shown clearly in the three-dimensional contact height mode AFM micrograph in Figure 4C.

The formation of fibrillated nanostructures by supramolecular assembling was also realized within a polypropylene matrix resulting in the formation of a second interconnected phase consisting of nanofibrils which are dispersed very effectively within the polymer matrix. Due to the rapid disassembling/reassembling of such supramolecular structures, they are not likely to reinforce the polymer matrix. However, nanostructure formation in the matrix of Thermoplast could result in nucleation of polymer crystallization.

B. Nucleation of Polypropylene Crystallization.

As a rule nucleating agents, which are added during melt processing of semicrystalline polymers, provide nuclei for crystallization, thus enhancing crystallization rate, decreasing spherulite size, and increasing crystallization temperature. During injection molding higher degree of crystallinity translates into improved stiffness, frequently accompanied by somewhat reduced toughness.^{6–10} Provided that the superstructures are small enough and that the dispersion of the nucleating agents is homogeneous, nucleation can afford improved optical clarity due to the presence of much smaller spherulites. Such nucleating agents are known as clarifiers. An important class of clarifiers used in polypropylene processing represent substituted dibenzylidene sorbitols, which are known to produce nanofibrillated network superstructures within the polypropylene matrix.^{6,10,32} While 1,3,2,4-dibenzylidenesorbitol (DBS)⁹ melts at 220 °C, more effective 1,3,2,4-dibenzylidenesorbitols with alkyl substitution of the aromatic ring have been introduced such as 1,3,2,4-bis(*p*-methylbenzylidene)sorbitol (MDBS),³³ melting at 245 °C, and 1,3,2,4-bis(*p*-ethylbenzylidene)sorbitol (EDBS), also known as "NC4",^{34,35} melting at 230 °C. For special applications of polypropylene processing at temperatures above 240 °C, 1,3,2,4-bis(3,4-dimethylbenzylidene)sorbitol, known as "Millad 3988", melting at 270 °C, has been developed. In addition to sorbitol derivatives, a variety of other nucleating agents are available for polypropylene, e.g. talcum, sodium benzoate, and 4-biphenylcarboxylic acid.^{7,8}

Most developments of nucleating agents are conducted empirically. An efficiency scale, proposed by Wittmann and co-workers, used crystallization of the self-nucleated as reference for nucleated polypropylene crystallization.⁸ A simple test for efficiency of nucleating agents effectiveness determines the increase of the crystallization temperature with respect to the same polymer in the absence of nucleating agent when the polymer crystallizes from the melt after heating it to 220 °C.^{9,33} For comparison of various nucleating agents, polypropylene and nucleating agent were blended to-

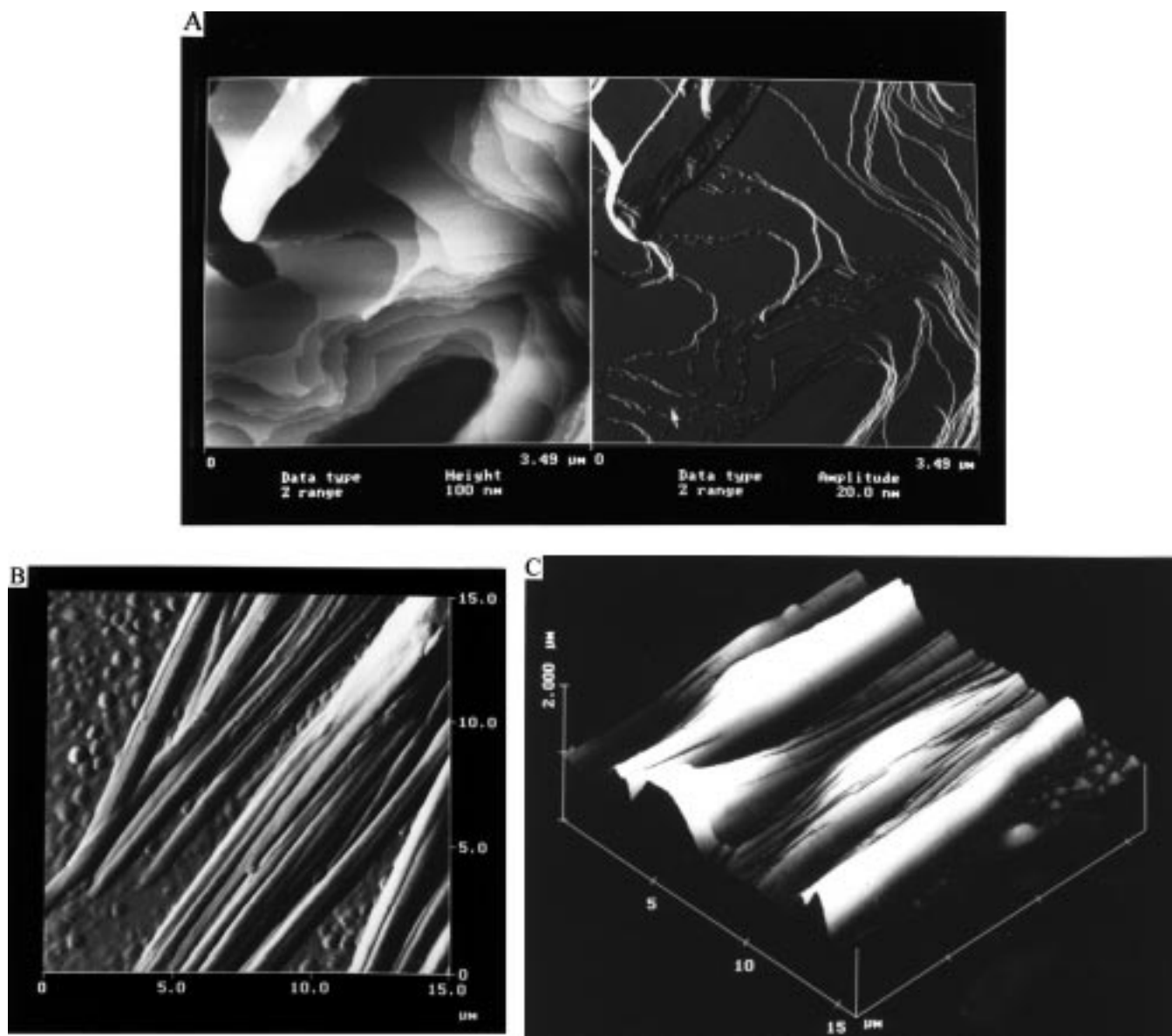


Figure 4. AFM micrographs of O-TP (A) (left, tapping height mode; right, tapping amplitude mode) and O-BA/O-TP assembly in contact deflection mode (B) and in contact height mode (C). O-BA/O-TP assembly samples were prepared by melt blending.

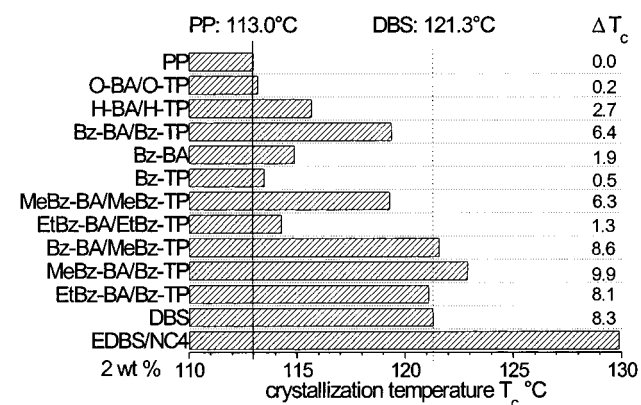


Figure 5. Performance of nucleating agents in polypropylene crystallization as determined by the difference of crystallization temperatures ΔT_c of polypropylene in absence and presence of nucleating agents (2 wt %).

gether in hot xylene, precipitated in supercooled acetone, dried, and investigated by means of thermal analysis (DSC).²⁶ The increases in melting crystalliza-

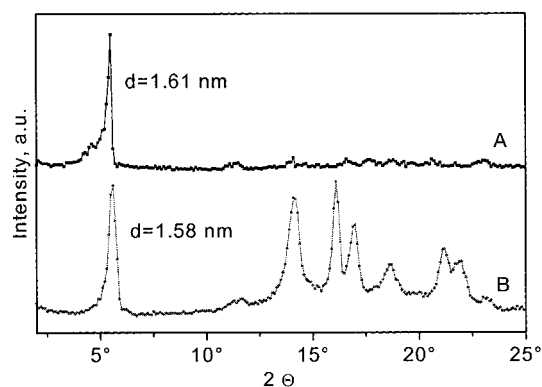


Figure 6. WAXS traces of MeBz-BA/Bz-TP (A) and polypropylene containing 10 wt % MeBz-BA/Bz-TP (B).

tion temperature, measured by cooling PP melts from 220 °C at 10 K/min, are graphically displayed for various nucleating agents in Figure 5. Interestingly, neither BA nor TP components act as nucleating agents. Only TP/BA self-assemblies appear to be effective with effectiveness increasing significantly as a function of the

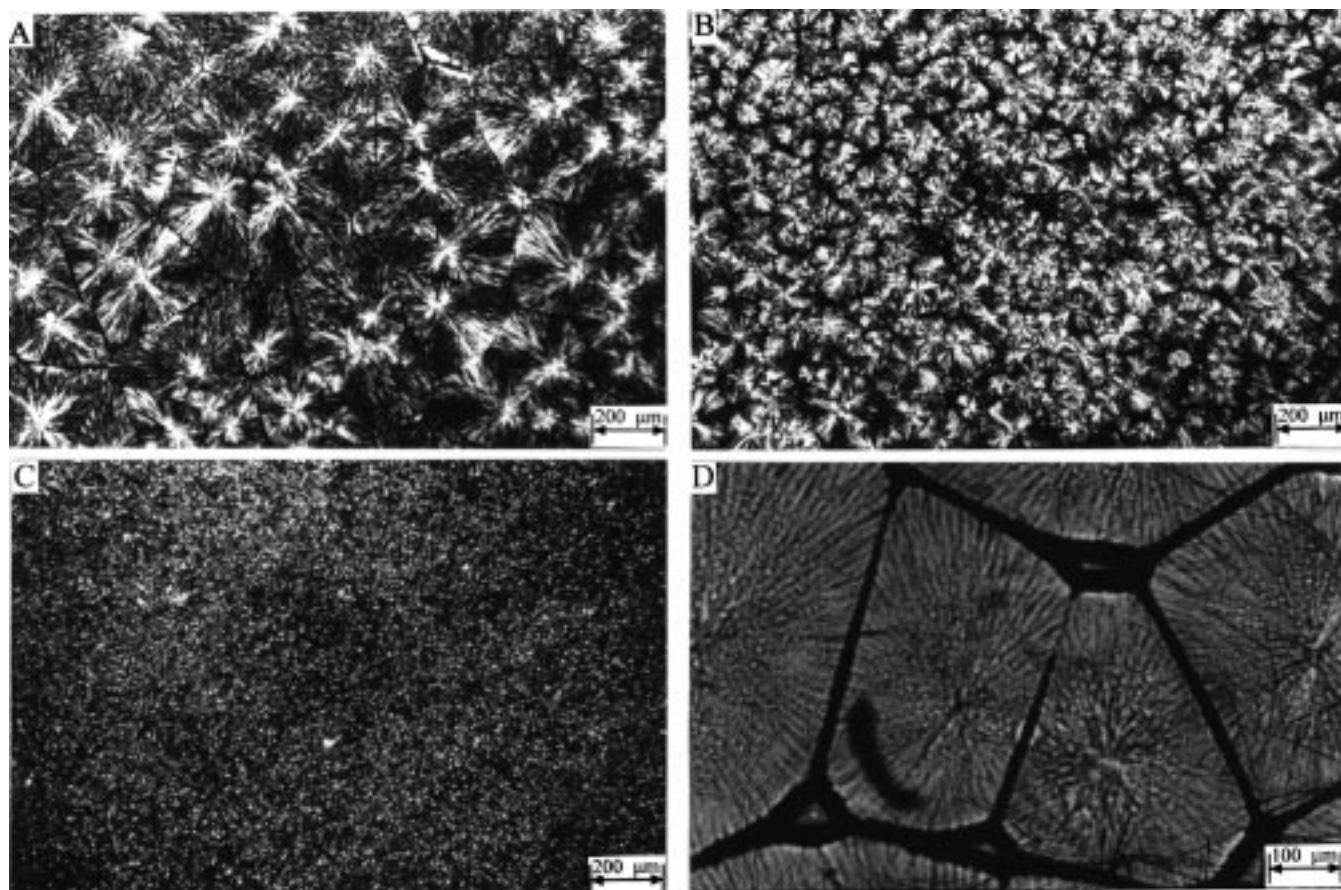


Figure 7. Crossed-polarized light microscopic images of polypropylene (A), polypropylene containing 2 wt % O-BA/O-TP (B) and the corresponding image with higher magnification (D), and polypropylene containing 2 wt % Bz-BA/Bz-TP (C). All samples were allowed to crystallize at 136 °C.

substituent type with alkyl-substituted benzyl > benzyl \gg hexadecyl \gg octyl.

For all BA/TP assemblies microscopic investigations revealed the formation of nanostructure formation within the polypropylene matrix. This is illustrated by the WAXS diagrams, displayed in Figure 6, for PP containing 10 wt % of MeBz-BA/Bz-TP. Both bulk MeBz-BA/Bz-TP and MeBz-BA/Bz-TP, formed during polypropylene blend formation, exhibited similar layered structures with interlayer distance of 1.61 and 1.58 nm, respectively. Thermal analysis of solution blends of polypropylene with various BA/TP showed the presence of the respective BA/TP assembly. The DSC traces showed melting of polypropylene first, followed by melting of the individual components and immediately afterward by crystallization of the corresponding BA/TP assembly, which melted at much higher temperatures well above 220 °C in the case of benzyl substitution (cf., Table 1). There was no evidence for the presence of residual components, which would not be effective as nucleating agents according to Figure 5.

It was possible to visualize formation of nanofibrillated BA/TP assemblies in the polypropylene matrix for octyl-, hexadecyl-, as well as benzyl-substituted compounds using cross-polarized light microscopy because the assemblies represented fairly large superstructures. In Figure 7 it is apparent that during isothermal crystallization needlelike features indicate the occurrence of nanofibrils resulting from BA/TP assembly. In fact, transcrystallization of polypropylene onto such nanofibrils was detected as the origin of nucleation. Clearly, the benzyl-substituted Bz-BA/Bz-TP was much

more effective with respect to O-BA/O-TP in accord with the DSC results displayed in Figure 5.

The performance of the benzyl-substituted Bz-BA/Bz-TP assembly in polypropylene nucleation was improved further by introducing alkyl substituents in the aromatic ring and using Bz-BA and Bz-TP blends with different alkyl substitution patterns. With MeBz-BA/Bz-TP it was possible to increase ΔT_c and surpass that of DBS, although the performance of EDBS/NC4 blends with ΔT_c of 16.9 °C was not matched. Although it is not clear why benzyl-substituted assemblies give better performance with respect to *n*-alkyl-substituted assemblies, there exists a correlation of ΔT_c with interlayer distance within the family of the benzyl-substituted BA/TP assemblies. As is apparent in Figure 8, maximum performance was observed for interlayer spacing of 1.61 nm. It should be noted that the same interlayer spacing of *n*-alkyl-substituted assemblies give much smaller ΔT_c . It appears likely that introducing two alkyl substituents, similar to substituted dibenzylidene sorbitol derivatives, may lead to further improvements in polypropylene nucleation obtained with Bz-BA/Bz-TP assemblies.

To study the influence of BA/TP assembly nucleating agents on polymer properties, especially stiffness as determined by the Young's modulus, polypropylene was extruded and injection molded in the presence of 0.1, 0.25, 0.5, 1 and 2 wt % of BA/TP nucleating agents. The results are listed in Table 2. While MeBz-BA/Bz-TP and Bz-BA/MeBz-TP addition did not impair impact strength, it afforded significantly higher stiffness, which is similar to that of polypropylene nucleated with DBS at concen-

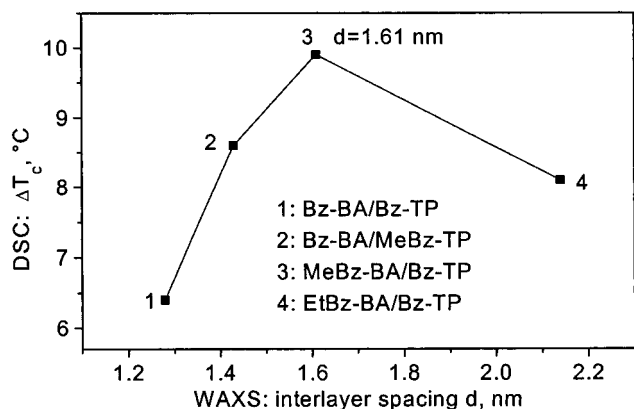


Figure 8. Influence of interlayer spacing of Bz-BA/Bz-TP assemblies, modified by varying the alkyl substituent at the aromatic rings.

Table 2. Mechanical Properties of Injection Molded Polypropylene Blends

nucleating agent	content (wt %)	Young's modulus (MPa)	yield stress (MPa)	impact strength (kJ/m ²)
iPP 100%	—	1310 ± 40	31.7 ± 0.3	2.2 ± 0.1
MeBz-BA/Bz-TP	0.1	1400 ± 40	32.1 ± 0.3	2.5 ± 0.1
MeBz-BA/Bz-TP	0.25	1450 ± 40	32.1 ± 0.3	2.6 ± 0.1
MeBz-BA/Bz-TP	0.5	1470 ± 40	32.3 ± 0.3	2.8 ± 0.1
MeBz-BA/Bz-TP	1	1490 ± 50	32.5 ± 0.3	2.9 ± 0.1
MeBz-BA/Bz-TP	2	1530 ± 50	32.7 ± 0.3	2.9 ± 0.1
Bz-BA/MeBz-TP	0.1	1400 ± 40	32.2 ± 0.3	2.4 ± 0.1
Bz-BA/MeBz-TP	0.25	1500 ± 50	32.3 ± 0.3	2.5 ± 0.1
Bz-BA/MeBz-TP	0.5	1510 ± 50	32.4 ± 0.3	2.5 ± 0.1
Bz-BA/MeBz-TP	1	1520 ± 50	32.5 ± 0.3	2.7 ± 0.1
Bz-BA/MeBz-TP	2	1520 ± 50	32.9 ± 0.3	2.7 ± 0.1
DBS ³⁶	0.1	1470 ± 40	33.2 ± 0.3	1.9 ± 0.1
DBS ³⁶	0.25	1560 ± 50	33.9 ± 0.3	1.8 ± 0.1
DBS ³⁶	0.5	1640 ± 50	34.6 ± 0.4	1.7 ± 0.1

trations usually applied in industrial practice. In view of the fairly large superstructures it is not surprising that BA/TP assemblies do not qualify as polypropylene clarifiers.

Conclusion

Supramolecular assembly of complementary tectonics such as derivatives of barbiturate (BA) and 2,4,6-triaminopyrimidine (TP) offer an attractive potential for preparation of gels and thermoplastic polymers such as polypropylene with nanoscale superstructures. Supramolecular superstructure formation is achieved even at very small contents of BA and TP components, which self-assemble very rapidly when BA and TP derivatives melt in polypropylene and form adducts with much higher melting temperatures. Due to the rapid disassembling/reassembling of hydrogen bridges in the polymer backbone, such nanofibers do not reinforce the polypropylene matrix as expected for corresponding nanofibers where monomeric units are covalently linked together. However, as will be presented later, it is possible to combine supramolecular assembly with cross-linking reaction within such fibers to afford formation of much stronger nanofibers in the polymer matrix. The nucleating efficiency of this new class of two-component nucleating agent is dependent upon the interlayer distance of such nanofibrils as well as the substitution type and substitution pattern of BA and TP. Models describing nucleation must be refined to find an explanation for this behavior and to take into account the role of the surface composition of nanofibrils in the nucleation of polypropylene crystallization.

Acknowledgment. The authors thank the Deutsche Forschungsgemeinschaft and the "Sonderforschungsbereich 428" for supporting this research.

References and Notes

- (1) Lehn, J. M. *Supramolecular Chemistry – Concepts and Perspectives*; Verlag Chemie: Weinheim, 1995; Chapter 9, p 139.
- (2) Simard, M.; Su, D.; Wuest, J. D. *J. Am. Chem. Soc.* **1991**, *113*, 4696.
- (3) Wuest, J. D. In *Mesomolecules – from Molecules to Materials*; Mendenhall, G. D., Greenberg, A., Liebman, J. F., Eds.; Chapman & Hall: New York, 1995; Chapter 4, p 107.
- (4) Sijbesma, R. P.; Beijer, F. H.; Brunsveld, L.; Folmer, B. J. B.; Hirschberg, J. H. K. K.; Lange, R. F. M.; Lowe, J. K. L.; Meijer, E. W. *Science* **1997**, *278*, 1601.
- (5) Terech, P.; Weiss, G. *Chem. Rev.* **1997**, *97*, 3133.
- (6) Shepard, T. A.; Delsorbo, C. R.; Louth, R. M.; Walborn, J. L.; Norman, D. A.; Harvey, N. G.; Spontak, R. J. *J. Polym. Sci., Polym. Phys.* **1997**, *35*, 2617.
- (7) Binsbergen, F. L. *Polymer* **1970**, *11*, 253.
- (8) Fillon, B.; Thierry, A.; Lotz, B.; Wittmann, J. C. *J. Therm. Anal.* **1994**, *42*, 721.
- (9) Fillon, B.; Lotz, B.; Thierry, A.; Wittmann, J. C. *J. Polym. Sci., Polym. Phys.* **1993**, *31*, 1395.
- (10) Smith, T. L.; Masilamani, D.; Bui, L. K.; Khanna, Y. P.; Bray, R. G.; Hammond, W. B.; Curran, S.; Belles, J. J.; Bindercastelli, S. *Macromolecules* **1994**, *27*, 3147.
- (11) Bloomfield, J. J. *J. Org. Chem.* **1961**, *26*, 4112.
- (12) Beckhaus, H. D.; Dogan, B.; Pakusch, J.; Verevkin, S.; Rüchardt, C. *Chem. Ber.* **1990**, *123*, 2153.
- (13) Milart, P.; Sepiol, J. Z. *Naturforsch.* **1986**, *41b*, 371.
- (14) Nanjo, K.; Suzuki, K.; Sekiya, M. *Chem. Pharm. Bull.* **1977**, *25*, 2396.
- (15) Sommer, R.; Müller, E.; Neumann, W. P. *Liebigs Ann. Chem.* **1968**, *718*, 11.
- (16) Russel, B.; Hitchings, G. H. *J. Am. Chem. Soc.* **1952**, *74*, 3443.
- (17) Lehn, J. M.; Mascal, M.; Decian, A.; Fischer, J. *J. Chem. Soc., Chem. Commun.* **1990**, 479.
- (18) Ram, V. J.; Nath, M. *Indian J. Chem.* **1994**, *33*, 1048.
- (19) Staudinger, H.; Kern, W. *Chem. Ber.* **1933**, *66*, 373.
- (20) Wong, O.; McKeown, R. H. *J. Pharm. Sci.* **1988**, *77*, 926.
- (21) Rosatzin, T.; Holy, P.; Seiler, K.; Rusterholz, B.; Simon, W. *Anal. Chem.* **1992**, *64*, 2029.
- (22) Fischer, E.; Diltthey, A. *Liebigs Ann. Chem.* **1904**, *335*, 334.
- (23) Levesque, D. L.; Wang, E. C.; Wei, D. C.; Tzeng, C. C.; Panzica, P. *J. Heterocycl. Chem.* **1993**, *30*, 1399.
- (24) Tate, J. V.; Tinnerman, W. N.; Jurevics, V.; Jeskey, H.; Biehl, E. R. *J. Heterocycl. Chem.* **1986**, *23*, 9.
- (25) Le Corre, M.; Gheerbrant, E.; Le Deit, H. *J. Chem. Soc., Chem. Commun.* **1989**, *5*, 313.
- (26) Puig, C. C.; Hill, M. J.; Barham, P. J. *Polymer* **1993**, *14*, 3117.
- (27) Drain, C. M.; Fischer, R.; Nolen, E. G.; Lehn, J. M. *J. Chem. Soc., Chem. Commun.* **1993**, 243.
- (28) Zerkowski, J. A.; Seto, C. T.; Wierda, D. A.; Whitesides, G. M. *J. Am. Chem. Soc.* **1990**, *112*, 9025.
- (29) Simanek, E. E.; Li, X.; Choi, I. S.; Whitesides, G. M. In *Comprehensive Supramolecular Chemistry*; Lehn, J. M., Ed.; Pergamon Press: Oxford, 1996; Vol. 9, Chapter 17, p 595.
- (30) Russell, K. C.; Leize, E.; Vandorsselaer, A.; Lehn, J. M. *Angew. Chem., Int. Ed. Engl.* **1995**, *34*, 209.
- (31) Hanabusa, K.; Miki, T.; Taguchi, Y.; Koyama, T.; Shirai, H. *J. Chem. Soc., Chem. Commun.* **1993**, 1382.
- (32) Thierry, A.; Straupe, C.; Lotz, B.; Wittmann, J. C. *Pol. Commun.* **1990**, *31*, 299.
- (33) Sterzynski, T.; Lambla, M.; Crozier, H. *Adv. Polym. Technol.* **1994**, *13*, 25.
- (34) Schlotmann, R.; Walker, R. *Kunststoffe* **1996**, *86*, 1002.
- (35) Becker, R. F.; Burton, L. P. J.; Amos, S. E. In *Polypropylene Handbook*; Moore, E. P., Ed.; Hanser Verlag: München, 1996; Chapter 4, p 190.
- (36) Data kindly obtained from Maier, R.-D., University of Freiburg.